The $\alpha2\beta1$ integrin inhibitor rhodocetin binds to the A-domain of the integrin $\alpha2$ subunit proximal to the collagen-binding site

Johannes A. EBLE*[1] and Danny S. TUCKWELL†[2]

*Institute of Physiological Chemistry and Pathobiochemistry, Münster University Hospital, Waldeyerstr. 15, 48149 Münster, Germany, and †School of Biological Sciences, University of Manchester, Stopford Building, Oxford Rd, Manchester, U.K.

Rhodocetin is a snake venom protein that binds to $\alpha2\beta1$ integrin, inhibiting its interaction with its endogenous ligand collagen. We have determined the mechanism by which rhodocetin inhibits the function of $\alpha2\beta1$. The interaction of $\alpha2\beta1$ with collagen and rhodocetin differed: Ca^{2+} ions and slightly acidic pH values increased the binding of $\alpha2\beta1$ integrin to rhodocetin in contrast with their attenuating effect on collagen binding, suggesting that rhodocetin preferentially binds to a less active conformation of $\alpha2\beta1$ integrin. The $\alpha2$A-domain [von Willebrand factor domain A homology domain (A-domain) of the integrin $\alpha2$ subunit] is the major site for collagen binding to $\alpha2\beta1$. Recombinant $\alpha2$A-domain bound rhodocetin, demonstrating that the A-domain is also the rhodocetin-binding domain. Although the interaction of $\alpha2\beta1$ with rhodocetin is affected by altering divalent cations, the interaction of the A-domain was divalent-cation-independent. The rhodocetin-binding site on the $\alpha2$A-domain was mapped first by identifying an anti-$\alpha2$ antibody that blocked rhodocetin binding and then mapping the epitope of the antibody using human–mouse $\alpha2$A-domain chimaeras; and secondly, by binding studies with $\alpha2$A-domain, which bear point mutations in the vicinity of the mapped epitope. In this way, the rhodocetin-binding site was identified as the $\alpha3$–$\alpha4$ loop plus adjacent α-helices. This region is known to form part of the collagen-binding site, thus attaining a mainly competitive mode of inhibition by rhodocetin.

Key words: A-domain, competitive inhibition, conformation, $\alpha2\beta1$ integrin.

INTRODUCTION

Among cell-adhesion molecules, integrins form a large family comprising 24 receptors of different ligand specificity (see [1,2] for reviews). Integrins consist of two non-covalently associated subunits, α and β. Integrins which contain the $\beta1$ subunit are mainly receptors for proteins of the extracellular matrix, such as collagen, laminin and fibronectin. Collagen-binding integrins, $\alpha1\beta1$, $\alpha2\beta1$, $\alpha10\beta1$ and $\alpha11\beta1$, form a subset within the integrin family [3–6]. Their α subunits contain an additional domain of about 200 amino acids. This insertion domain (I-domain) is also called A-domain [von Willebrand factor (vWF) domain A homology domain], because of its similarity to the latter. It is exposed on top of the heterodimeric integrin and is responsible for collagen binding [7,8]. Integrin binding to collagen indispensably requires the triple-helical conformation of the collagenous ligand (see [9,10] and refs in [2]).

Considerable insights into the molecular mechanism of integrin–ligand interaction have recently been provided by X-ray crystal-structure analysis of integrin–ligand complexes ([11,12], and reviewed in [13,14]). Centrally located within the collagen-binding groove of the $\alpha2$A-domain (A-domain of the integrin $\alpha2$ subunit) is a divalent cation, which is essential for collagen binding. It is complexed by residues from three different loops of the A-domain, thus forming a MIDAS (metal-ion-dependent adhesion site) [15]. The collagen molecule is bound both by the bridging divalent cation and by hydrogen bonds to residues on the top surface of the A-domain [12]. Collagen binding induces a conformational shift within the $\alpha2$A-domain, involving some α-helices which flank the central β-sheet of the A-domain on both sides [14,15]. This conformational change is likely to be transferred to the rest of the integrin ectodomain [13,14] and eventually to the cytoplasmic domains, which trigger intracellular signals as a response to integrin-mediated cell attachment [1].

Naturally occurring integrin inhibitors have been found in venoms of snakes, leeches and insects. Most of the known integrin inhibitors are disintegrins [16], which bear a functional Arg-Gly-Asp (RGD) sequence in a flexible loop. Thus they block RGD-dependent integrins, especially the integrin $\alpha IIb\beta3$ on the platelet surface. However, some RGD-independent integrin inhibitors have been discovered, which target collagen-binding integrins. Rhodocetin from *Calloselasma rhodostoma* [17] and Jararhagin from *Bothrops jararaca* [18,19] bind $\alpha2\beta1$ integrin and inhibit its binding to collagen. Integrin $\alpha2\beta1$ is the only collagen-binding integrin on platelets and, together with the non-integrin collagen receptor GPVI, triggers collagen-induced platelet activation and aggregation [20]. Blockage of $\alpha2\beta1$ integrin by rhodocetin therefore impairs blood clotting [21]. However, $\alpha2\beta1$ is not only found in platelets but is also present in numerous other cell types, where it is responsible for a variety of different cellular responses to collagen [22]. In a previous paper, we found rhodocetin to antagonize diverse $\alpha2\beta1$ integrin-related functions [23].

In the present study, we determined the mechanism by which rhodocetin interferes with $\alpha2\beta1$ integrin binding to collagen. Rhodocetin binds to the $\alpha2$A-domain. The $\alpha3$–$\alpha4$ loop and its adjacent α-helices comprise the putative rhodocetin-binding site of

Abbreviations used: ABTS, 2,2′-azinobis-(3-ethylbenzothiazoline-6-sulphonic acid); vWF, von Willebrand factor; A-domain, vWF domain A homology domain; $\alpha2$A-domain, A-domain of the integrin $\alpha2$ subunit; GST, glutathione S-transferase; GST-$\alpha2$A, recombinant GST-tagged $\alpha2$A-domain; HBS, Hepes-buffered saline; mAb, monoclonal antibody; MIDAS, metal-ion-dependent adhesion site; TBS, Tris-buffered saline.

[1] To whom correspondence should be addressed (e-mail eble@uni-muenster.de).

[2] Present address: F2G Ltd., The Incubator Building, Grafton Street, Manchester M13 9XX, U.K.

the α2A-domain. This loop also forms part of the collagen-binding site. Therefore, probably because of steric hindrance, rhodocetin competes with collagen for the $\alpha2\beta1$ integrin. Our results also suggest that rhodocetin preferentially recognizes the less-active conformation of the A-domain.

EXPERIMENTAL

Materials

The purification of rhodocetin from *C. rhodostoma* venom has been described recently [17]. The crude toxin of *C. rhodostoma* was provided by Dr Margarete Schwarz (Knoll Pharmaceuticals, Ludwigshafen, Germany). Soluble $\alpha2\beta1$ integrin was recombinantly expressed in an insect-cell expression system and purified as described previously [17]. The rat mAb (monoclonal antibody) 9EG7, directed against the integrin $\beta1$ subunit, was isolated from the hybridoma supernatant according to standard procedures. The 9EG7 hybridoma cells were kindly provided by Dr D. Vestweber (University of Münster, Germany). The murine mAbs, 6S6 and JB1A, which function by blocking mAbs against the integrin $\beta1$ subunit, were purchased from Chemicon (Temecula, CA, U.S.A.). Bacterial expression and purification of the GST-α2A (glutathione S-transferase-tagged α2A-domain) has been described previously [7]. The murine mAbs JA202, JA203, JA208, JA215, JA218 and JA221, directed against the human α2A-domain, were generated as described in a previous paper [24].

Binding of soluble $\alpha2\beta1$ integrin to rhodocetin and type I collagen

Rhodocetin in 20 mM sodium phosphate (pH 6.5), 70 mM NaCl and type I collagen in 0.1 M acetic acid was coated on to microtitre plates at 4 °C overnight. After washing three times with HBS [Hepes-buffered saline: 50 mM Hepes/NaOH (pH 7.0)/150 mM NaCl] (pH 7.1) or TBS [Tris-buffered saline: 50 mM Tris/HCl (pH 7.4)/150 mM NaCl] (pH 7.4), each containing 2 mM $MgCl_2$, wells were blocked with 1 % BSA in the same buffer (1 % BSA/HBS/Mg or 1 % BSA/TBS/Mg) for 2 h at room temperature (20 °C). Soluble $\alpha2\beta1$ integrin was diluted in 1 % BSA/HBS/Mg or 1 % BSA/TBS/Mg, and additives, e.g. 1 mM $MnCl_2$, integrin-activating or -inhibiting mAbs, were added as specified. To determine the optimum pH of the integrin–ligand interaction, ampholines (pH 4–10; Amersham Biosciences, Freiburg, Germany) at 40 mg/ml were used as buffering agents and their pH adjusted to the indicated pH values. The $\alpha2\beta1$ integrin solution was incubated for 2 h in the coated wells. Non-bound integrin was washed off the plate twice with HBS (pH 7.4), containing 2 mM $MgCl_2$ and 1 mM $MnCl_2$. The bound integrin was fixed to the wells with 2.5 % (v/v) glutaraldehyde solution in the same buffer for 10 min at room temperature, and quantified by ELISA using a rabbit antiserum directed against the integrin $\beta1$ subunit and alkaline phosphatase-conjugated antibodies raised against rabbit IgG (Sigma, Deisenhofen, Germany), diluted 1:400 and 1:600 respectively in BSA/TBS/Mg buffer for 1.5 h each. Both the antibody incubation step and the final development step were preceded by three washes with TBS/Mg buffer. The ELISA was developed with *p*-nitrophenyl phosphate (Sigma) in a 0.1 M glycine buffer (pH 10.4), supplemented with 1 mM $MgCl_2$ and zinc acetate. The dye reaction was stopped by the addition of a 1.5 M NaOH solution, and the absorbance was measured in an ELISA reader (Dynatech, Germany) at 405 nm versus 595 nm. Linearization of titration curves and determination of apparent affinity constants were performed as described by Heyn and Weischet [27].

Binding of GST-α2A to immobilized rhodocetin and type I collagen

Rhodocetin and type I collagen were coated onto microtitre plates, as described above. GST-α2A and the GST protein were diluted in 1 % BSA/HBS (pH 7.1)/2 mM $MgCl_2$, supplemented with one of the following: 1 mM $MnCl_2$; 1 mM $MnCl_2$ and the activating mAb 9EG7 with 2 mM $CaCl_2$ or with 10 mM EDTA. The binding partners were incubated with the immobilized proteins for 2 h at room temperature. After washing the wells with HBS (pH 7.1) and 2 mM $MgCl_2$, supplemented with the respective additives, the bound GST-α2A protein was fixed with 2.5 % glutaraldehyde in HBS (pH 7.4), 2 mM $MgCl_2$ and 1 mM $MnCl_2$ for 10 min and its amount quantified in one of the two alternative ELISA-like procedures. First, the GST-tagged α2A-domain was detected by polyclonal rabbit antibodies directed against the GST moiety (Molecular Probes, Leiden, The Netherlands) and, subsequently, by alkaline-phosphate-conjugated antibodies raised against rabbit antibodies (Sigma), both diluted at 1:600 in 1 % BSA, TBS (pH 7.4) and 2 mM $MgCl_2$. Secondly, the GST-α2A was detected by the mAb JA218, added to GST-α2A during the binding step. The complex of bound GST-α2A with JA218 was then quantified by biotinylated sheep antibodies raised against mouse IgG (Amersham Biosciences) and, subsequently, by alkaline-phosphatase-coupled extravidin (Sigma), diluted at 1:500 and 1:1000 respectively in 1 % BSA, TBS (pH 7.4) and 2 mM $MgCl_2$. The mAb JA218 does not interfere with either rhodocetin or collagen binding to the integrin (see Figure 6). Furthermore, the second detection system with mAb JA218 allowed comparative binding studies with both the soluble $\alpha2\beta1$ integrin and the α2A-domain. The ELISA was developed as described above. The rat mAb 9EG7 did not interfere with any of the detection systems.

Epitope mapping of mAb directed against the α2A-domain

The human–mouse chimaeric recombinant α2A-domain constructs used to map the anti-α2 mAbs have been described in [28]. The mAb of the JA series used in our studies belong to a panel of 21 mAbs directed against the α2A-domain, JA201–JA221, the generation of which has been described in a previous paper [24]. Assays to measure antibody binding to recombinant GST-fusion proteins of the α2A-domain were performed as described by Brookman et al. [29]. Immunolon 4 microtitre plates were coated with 100 μl of 5 μg/ml fusion protein in PBS, containing 0.9 mM Ca^{2+} and 0.5 mM Mg^{2+}, overnight at 4 °C. Wells were then washed twice with 200 μl PBS and blocked with 2 % (w/v) fat-free milk powder in PBS for 1 h at 4 °C. Wells were then washed twice with 200 μl of 0.1 % (v/v) Tween 20, PBS (washing buffer) and 100 μl of antibody diluted in 0.5 % (w/v) milk powder in washing buffer added for 2 h at 4 °C. After unbound antibodies were removed by two washing steps with 200 μl washing buffer, peroxidase-conjugated antibodies raised against either mouse IgG (Dako, Hamburg, Germany) or sheep IgG [recognizing the sheep antibodies raised against GST; diluted in 0.5 % (w/v) milk powder in washing buffer] were added for 2 h at 4 °C. After three washes with washing buffer, the colour was developed by the addition of ABTS [2,2′-azinobis-(3-ethylbenzothiazoline-6-sulphonic acid)] and measured at 405 nm.

Generation and production of recombinant GST-α2A mutants

The generation of the pGEX-2T/wild-type α2A-domain construct, encoding the GST-fusion protein of the wild-type α2A-domain, has been described previously [7]. Mutagenesis of this construct was carried out using the QuikChange site-directed

mutagenesis kit (Stratagene, La Jolla, CA, U.S.A.). Mutagenesis reactions were performed according to the manufacturer's instructions using pGEX-2T/wild-type α2A-domain construct as template. The following complementary pairs of oligonucleotide primers were used to introduce the mutations: mutant I ($Asn^{154} \rightarrow$ Ala), 5′-GTGTGTGATGAATCAGCTAGTATTTATCCTTGGG-3′, 5′-CCCGATAAATACTAGCTGATTCATCACACAC-3′; mutant II ($Asn^{196} \rightarrow$ Ala, $Asn^{198} \rightarrow$ Ala), 5′-CCAAGAGTTGTGTTT-GCCTTGGCCACATATAAAACC-3′, 5′-GGTTTTATATGTGG-CCAAGGCAAACACAACTCTTGG-3′; mutant III ($Asp^{219} \rightarrow$ Ala, $Leu^{220} \rightarrow$ Ala, $Asn^{222} \rightarrow$ Ala), 5′-CAATATGGTGGGGCC-GCCACAGCCACATTCGG-3′, 5′-CCGAATGTGGCTGTGGC-GGCCCCACCATATTG-3′; mutant IV ($Arg^{231} \rightarrow$ Ala, $Tyr^{233} \rightarrow$ Ala, $Ser^{236} \rightarrow$ Ala), 5′-CAATTCAATATGCAGCAAAAGCTGC-CTATGCAGCAGCTTCTG-3′, 5′-CAGAAGCTGCTGCATAG-GCAGCTGTTGCTGCATATTGAATTG-3′; mutant V ($Glu^{256} \rightarrow$ Ala, $His^{258} \rightarrow$ Ala), 5′-CTAACTGACGGTGCATCAGCTGATG-GTTCAATG-3′, 5′-CATTGAACCATGAGCTGATGCACCGT-CAGTTAC-3′; and mutant VI ($Ser^{261} \rightarrow$ Ala, $Lys^{264} \rightarrow$ Ala), 5′-GAATCACATGATGGTGCAATGTTGGCAGCTGTGATTG-ATC-3′, 5′-GATCAATCACAGCTGCCAACATTGCACCATCA-TGTGATTC-3′. Primers were obtained from MWG Biotech (Milton, Keynes, U.K.).

The products of the mutagenesis reactions *in vitro* were transfected into XL1-blue cells and the mutations verified by sequencing. Validated constructs were then used to transfect *Escherichia coli* strain DH5α for protein expression. Wild-type and mutant recombinant GST-α2A fusion proteins were produced and purified as described previously [7,24,30]. Mutants I and III lost binding activity when stored at 4 °C for some days. Since this instability was also observed for the GST-wild-type α2A fusion protein, albeit to a lesser extent, measurements were performed immediately after thawing the fusion proteins.

Binding curves of soluble $\alpha 2\beta 1$ integrin to CB3 in the presence and absence of rhodocetin

Soluble $\alpha 2\beta 1$ integrin was biotinylated with a 100-fold molar excess of sulpho-succinimidyl-6-biotinamido hexanoate (EZ-Link Sulfo NHS LC Biotin, Pierce, Bonn, Germany) for 2 h at 26 °C after dissolving in HBS, supplemented with 2 mM $MgCl_2$. Biotinylation was stopped by the addition of 20 mM Tris (pH 8.0), and excess biotinylation reagent was removed by dialysis. Biotinylation of soluble $\alpha 2\beta 1$ integrin did not alter its binding specificity or affinity.

A solution (280 μl) of biotinylated $\alpha 2\beta 1$ integrin [18 μg/ml of 0.1 % BSA in TBS (pH 7.4)/2 mM $MgCl_2$/1 mM $MnCl_2$; binding buffer] was mixed with various concentrations of the type IV collagen fragment CB3 (a gift from Dr K. Kühn, Max-Planck-Institut für Biochemie, Martinsried, Germany) [25,26] in the absence or presence of 32 nM rhodocetin, as well as in the presence of 10 mM EDTA (to determine the non-specific background signal), and incubated for 2 h at room temperature. Streptavidin–agarose (35 μl; Sigma), equilibrated with binding buffer, was added to each mixture and the incubation was continued for 1.5 h. Integrin-bound CB3, captured by streptavidin–agarose, was precipitated by centrifugation. The CB3 concentration in the supernatant represented the free CB3. The resin-bound integrin–CB3 complex was washed four times with binding buffer, either without or with EDTA, and bound CB3 was eluted with a 30 mM EDTA solution in 0.1 % BSA and TBS (pH 7.4) in a volume of 300 μl.

Concentrations of free and integrin-bound CB3 were quantified in a newly established sandwich ELISA. To this end, the murine mAb CIV22 directed against the type IV collagen fragment CB3 (provided by Dr B. Odermatt, Universitätsspital Zürich, Switzerland) was coated on to microtitre plates overnight at 4 °C. After two washing steps with TBS (pH 7.4), supplemented with 2 mM $MgCl_2$ (TBS/Mg buffer), non-specific protein-binding sites were blocked with 1 % BSA solution in TBS/Mg buffer. A calibration row of CB3, ranging from 3 to 0.1 nM including a CB3-free blank, and the CB3 solutions from the binding experiments, which were diluted appropriately, were plated on to the plate for 2 h at room temperature. After two washing steps with HBS (pH 7.4), CIV22-captured CB3 was fixed to the plate with 2.5 % glutaraldehyde in the same buffer. The amount of CB3 was then quantified by an ELISA procedure, using a polyclonal rabbit antiserum raised against CB3 and alkaline phosphatase-conjugated antibodies directed against rabbit IgG (Sigma), diluted to 1:300 and 1:600 respectively in 1 % BSA in TBS/Mg buffer. The ELISA was developed as described above. Concentrations for both free and integrin-bound CB3 were determined in duplicates. From the value pairs (bound versus free CB3), measured in the presence of 10 mM EDTA (Figure 8A), non-specific binding was calculated and was used to correct the value pairs measured in both the absence and presence of rhodocetin. Corrected values were plotted double reciprocally. Standard deviations were calculated from the original data using Gauss' law of error progression.

RESULTS

Rhodocetin is preferentially bound by $\alpha 2\beta 1$ integrin in the presence of Ca^{2+} ions and slightly acidic pH

To find the optimal binding conditions for rhodocetin binding to $\alpha 2\beta 1$ integrin, we studied their interaction in the presence of activators and attenuators of integrin function. Compared with the $\alpha 2\beta 1$ integrin-binding signal measured in the presence of TBS (pH 7.4) and 2 mM $MgCl_2$ (basic conditions), addition of integrin activators, e.g. Mn^{2+} ions and the mAb 9EG7 [31], and addition of integrin inhibitors, e.g. function blocking mAb against the integrin $\beta 1$ subunit, 6S6 and JB1A [32], as well as EDTA, affected the interaction of $\alpha 2\beta 1$ integrin with collagen, but had little or no effect on its binding to rhodocetin. However, Ca^{2+} ions had the opposite effect on $\alpha 2\beta 1$ integrin binding to rhodocetin compared with its binding to collagen (Figure 1A).

Another parameter influencing integrin–ligand interactions is pH. Integrin $\alpha 2\beta 1$ bound to its physiological ligand, type I collagen, only in a pH range > 6.5, with an optimum pH between 7.0 and 8.5. Under slightly acidic conditions, integrin binding to collagen decreased drastically (Figure 1B). In contrast, rhodocetin interacted with soluble $\alpha 2\beta 1$ integrin over a broad pH range, with an optimum pH between 5.5 and 7.0. Within this acidic pH range, the integrin remained intact as judged by ELISA detection with conformation-dependent mAbs (results not shown), but probably assumed an inactive conformation which was not capable of binding to type I collagen.

The divalent-cation dependence of $\alpha 2\beta 1$ integrin binding to rhodocetin, shown in Figure 1(A), was studied in detail. Titration of soluble $\alpha 2\beta 1$ integrin to immobilized rhodocetin demonstrated that $\alpha 2\beta 1$ integrin bound more avidly to rhodocetin in the presence of Ca^{2+} ions than in the presence of Mn^{2+} ions or EDTA (Figure 2). This is different from the inhibitory effects of Ca^{2+} ions on $\alpha 2\beta 1$ integrin binding to collagen. From the titration curve, an apparent affinity constant K_d for $\alpha 2\beta 1$ integrin binding to rhodocetin was calculated to be 1.6 nM in the presence of 2 mM Ca^{2+} ions. In the presence of EDTA and 1 mM Mn^{2+} ions, the K_d values increased to 12.9 and 13.2 nM, respectively.

These results indicate that rhodocetin binding to $\alpha 2\beta 1$ integrin is supported by Ca^{2+} ions, which are known to decrease the affinity

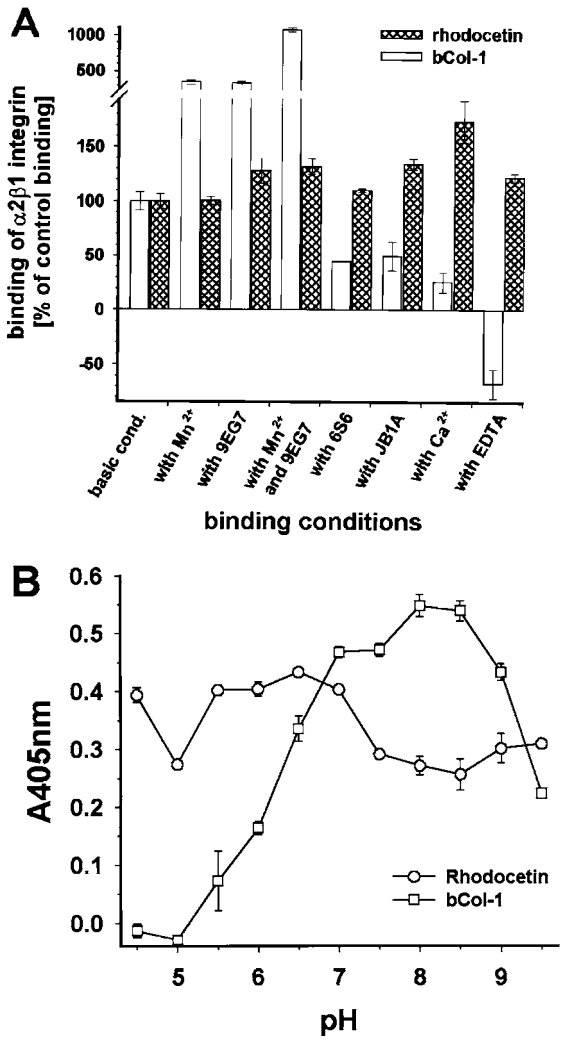

Figure 1 $\alpha2\beta1$ integrin binding to rhodocetin is regulated distinctly from its binding of type I collagen: effect of integrin activators and inhibitors, and effect of pH

(**A**) Rhodocetin (at 15 μg/ml) and type I collagen (at 30 μg/ml) were immobilized on microtitre plates and incubated with soluble $\alpha2\beta1$ integrin [12 μg/ml in 1 % BSA, HBS (pH 7.1) and 2 mM $MgCl_2$; basic condition], to which Mn^{2+} ions at 1 mM and/or the integrin activating mAb 9EG7, the integrin-blocking mAbs 6S6 and JB1A, Ca^{2+} ions at 2 mM or 10 mM EDTA were added. Both the activating and blocking antibodies are directed against the integrin $\beta1$ subunit and were added at a 2-fold molar excess to the integrin. (**B**) To immobilized rhodocetin (20 μg/ml) (○) and bovine type I collagen (10 μg/ml) (□), soluble $\alpha2\beta1$ integrin (9 μg/ml) was added in a 40 mg/ml ampholine-buffered saline (150 mM NaCl), containing either 2 mM $CaCl_2$ (binding to rhodocetin, ○) or 1 mM $MnCl_2$ and 90 nM 9EG7 (binding to type I collagen, □) for 2 h at room temperature. After removal of non-bound integrin by washing, bound $\alpha2\beta1$ was fixed with glutaraldehyde and detected with an antiserum against the human integrin $\beta1$ subunit by ELISA, as detailed in the Experimental section. Mean values and standard deviations from duplicate determinations are shown.

of $\alpha2\beta1$ integrin to type I collagen, presumably by inducing a conformational change within the integrin. Interestingly, rhodocetin seems to bind preferentially to this Ca^{2+} ions-induced, less-active conformation of the $\alpha2\beta1$ integrin.

Rhodocetin binds to the α2A-domain

One possible mechanism for the inhibitory action of rhodocetin on $\alpha2\beta1$ integrin is that the snake-venom component sterically

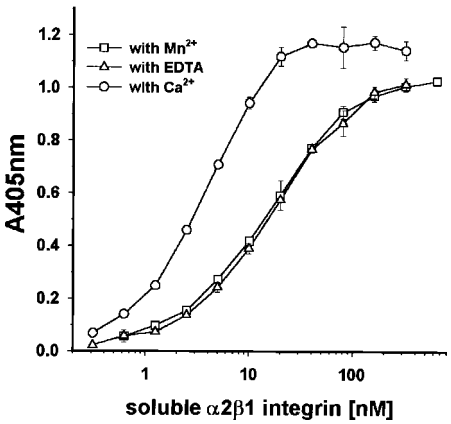

Figure 2 Titration of immobilized rhodocetin with soluble $\alpha2\beta1$ integrin binding

Rhodocetin (at 15 μg/ml) was coated onto microtitre plates at 4 °C, overnight, and incubated with various concentrations of soluble $\alpha2\beta1$ integrin in 1 % BSA, TBS (pH 7.4) and 1 mM $MgCl_2$ in the presence of either 1 mM Mn^{2+} ions (□), 10 mM EDTA (△) or 2 mM Ca^{2+} ions (○). The bound $\alpha2\beta1$ integrin was detected by rabbit antibodies directed against the integrin $\beta1$ subunit and, subsequently, by alkaline phosphatase-conjugated antibodies directed against rabbit IgG. Mean values and standard deviations were calculated from duplicate determinations and corrected for the respective background values, as measured on BSA-coated wells.

blocks the collagen-binding site of the integrin. It has been shown previously that the α2A-domain is the essential, if not the only, collagen-binding site within the integrin [7,8]. To test whether rhodocetin also recognizes the α2A-domain, we produced GST-α2A in a bacterial expression system. Soluble $\alpha2\beta1$ integrin and GST-α2A bound to immobilized rhodocetin (Figure 3), thus proving that rhodocetin interacts with the collagen-binding α2A-domain. In Figure 3(A), bound $\alpha2\beta1$ integrin was detected with a rabbit antiserum against the integrin $\beta1$ subunit, whereas bound GST-α2A and the control GST domain were detected with a rabbit antiserum against the GST tag. In Figure 3(B), both bound $\alpha2\beta1$ integrin and bound GST-α2A were quantified by the same mAb JA218 to obtain comparable results. No gross differences were observed between the two detection systems (Figure 3A versus Figure 3B). Binding of the GST-α2A to rhodocetin was specific, since the GST domain alone did not show any binding signal. Furthermore, binding of the GST-α2A to rhodocetin was generally higher than that of soluble $\alpha2\beta1$ integrin. Soluble $\alpha2\beta1$ integrin in its activated form showed a clear binding signal to collagen. However, the binding signals of GST-α2A, albeit applied at the same molar concentration as the entire integrin ectodomain heterodimer, were only slightly higher than the GST control (Figure 3A) or approached control levels, when detected with the mAb JA218 (Figure 3B). Higher concentrations of GST-α2A were required to demonstrate specific binding (see below, Figure 7B), suggesting that the isolated α2A-domain is less active for collagen binding than the entire $\alpha2\beta1$ integrin ectodomain. Binding of $\alpha2\beta1$ integrin to type I collagen was strongly increased by the activating antibody 9EG7, which is directed against integrin $\beta1$ subunit. The mAb 9EG7 did not affect GST-α2A binding to either rhodocetin or type I collagen (Figures 3A and 3B), ruling out a direct interaction of 9EG7 with the α2A-domain. Moreover, since the rat mAb 9EG7 did not interfere with any of the detecting antibodies (results not shown), its activation must be an indirect, conformational effect from the integrin $\beta1$ subunit to the α2A-domain.

$\alpha2\beta1$ integrin binding is regulated by divalent cations. As already seen in Figure 1(A), Mn^{2+} ions increase the binding signal

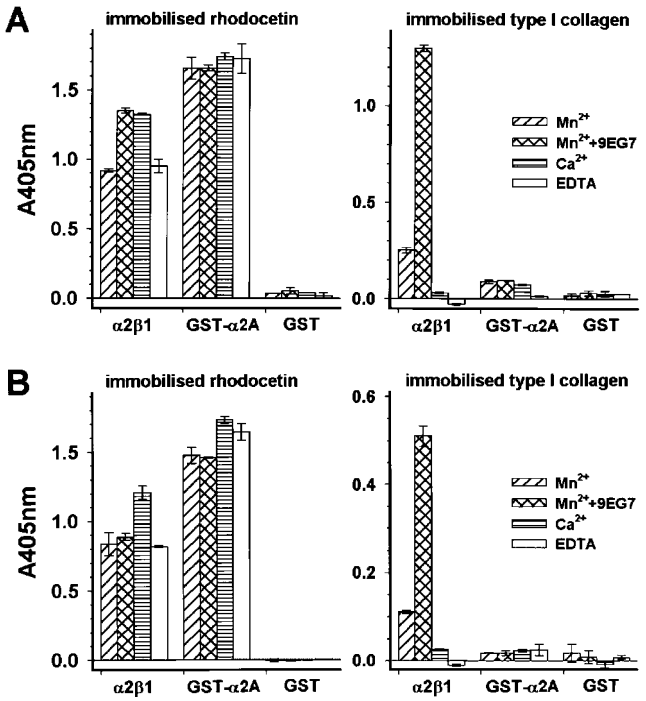

Figure 3 The α2A-domain contains the integrin binding site for rhodocetin

Rhodocetin (at 15 μg/ml) and type I collagen (at 30 μg/ml) were immobilized on microtitre plates. Equimolar concentrations (each 50 nM) of soluble $\alpha2\beta1$ integrin, the GST-α2A fusion protein and GST protein alone were added to the wells in the presence of 1 mM Mn^{2+} ions alone (hatched bars), or in combination with mAb 9EG7 (cross-hatched bars), or in the presence of 2 mM Ca^{2+} ions (horizontally striped bars) or 10 mM EDTA (open bars). Detection of bound protein was performed in two different ways: (**A**) bound $\alpha2\beta1$ integrin and GST-α2A were detected by antibodies raised against the integrin $\beta1$ subunit and against the GST moiety respectively. (**B**) To allow comparison of binding signals, bound $\alpha2\beta1$ integrin and GST-α2A were detected by mAb JA218 directed against the α2A-domain. Signals were corrected for non-specific binding of soluble $\alpha2\beta1$, GST-α2A and GST alone to BSA-coated wells under the same binding conditions. Mean values and standard deviations of duplicate determinations are shown.

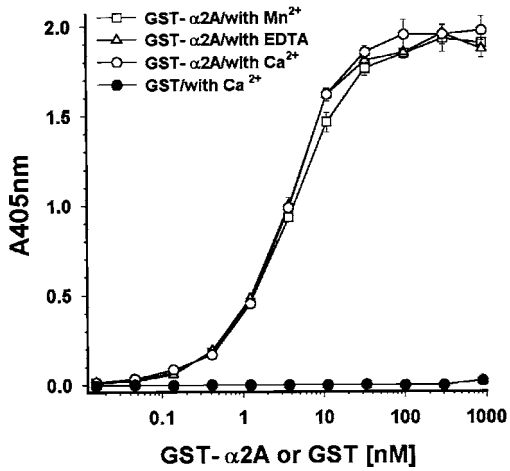

Figure 4 Titration of immobilized rhodocetin with GST-tagged integrin α2A-domain

Rhodocetin (at 15 μg/ml) was coated on microtitre plates at 4 °C overnight and incubated with various concentrations of GST protein alone (●) or GST-α2A fusion protein (open symbols), in the presence of either 1 mM Mn^{2+} ions (□), 10 mM EDTA (△) or 2 mM Ca^{2+} ions (○). Bound GST-tagged α2A and GST were detected by rabbit antibodies directed against the GST moiety and, subsequently, by alkaline phosphatase-conjugated antibodies directed against rabbit IgG. Mean values and standard deviations were calculated from duplicate determinations and corrected for the respective background values, measured on BSA-coated wells.

of soluble $\alpha2\beta1$ integrin to type I collagen but not to rhodocetin. Ca^{2+} ions influence binding to rhodocetin positively but influence binding to type I collagen negatively. In contrast, binding of the isolated α2A-domain to rhodocetin was not affected by these divalent cations, suggesting that the divalent-cation dependence of $\alpha2\beta1$ integrin binding to rhodocetin is imposed on the α2A-domain by the rest of the integrin ectodomain.

For a detailed analysis of the divalent cation-independent interaction of α2A-domain, immobilized rhodocetin was titrated with the GST-α2A fusion protein in the presence of 1 mM Mn^{2+} or 2 mM Ca^{2+} ions or EDTA (Figure 4). The apparent K_d value of 2.2 nM for GST-α2A binding to rhodocetin in the presence of Ca^{2+} ions did not significantly differ from the K_d values of 3.1 and 3.7 nM, measured in the presence of EDTA and Mn^{2+} ions respectively. In comparison, binding of the entire $\alpha2\beta1$ integrin ectodomain to rhodocetin was affected by divalent cations (Figure 2). At millimolar quantities, Ca^{2+} ions favoured rhodocetin binding and induced the less-active conformation of $\alpha2\beta1$ integrin. Conspicuously, in the presence of Ca^{2+} ions, both the entire $\alpha2\beta1$ integrin ectodomain and the α2A-domain bound to rhodocetin with similar affinity constants, suggesting that the isolated α2A-domain assumes the less-active conformation, which can be probed by rhodocetin.

Table 1 Epitope mapping of mAbs to the α2A-domain

The epitopes for mAbs JA215, JA218 and JA221 were mapped using human–mouse α2A-domain chimaeras [28]. The mutations introduced to convert stretches of human-to-mouse sequence are shown. Chimaeras exhibiting decreased binding of antibodies are given in bold. Microtitre plates were coated with 5 μg/ml wild-type or chimaeric α2A-domain and the binding of antibodies was measured. Binding of anti-GST antiserum to constructs was used to normalize the data between the α2A-domains. Data are means ± S.D. of duplicate determinations each from two independent experiments. Hu α2, wild-type human α2A-domain; Mo α2, wild-type mouse α2A-domain. D160E etc., $Asp^{160} \rightarrow$ Glu mutation etc.

	mAb		
Wild-type/chimaeric α2A-domain	JA215	JA218	JA221
Hu α2	100 ± 4.3	100 ± 5.6	100 ± 2.6
Mo α2	2.5 ± 3.8	−0.2 ± 0.4	−0.2 ± 1.1
D160E, E167V	94.4 ± 9.9	92.3 ± 7.3	98.7 ± 4.5
Q171T, T178K, G183A	101.3 ± 3.6	100.4 ± 9.0	100.3 ± 3.4
N190E, V193I, V194I	96.6 ± 4.2	98.5 ± 9.1	89.0 ± 2.6
T199D, Y200F, K201E	89.5 ± 6.4	89.7 ± 2.6	89.4 ± 3.0
E205D, I207V, V208Q, Q212E, S214R, Y216H	91.9 ± 7.0	87.2 ± 10.7	89.3 ± 6.8
G225R, Q228E, Y229F, K232D	102.8 ± 1.1	100.8 ± 7.4	**−0.3 ± 0.4**
A237Q, A238T, R234P, S244G	87.6 ± 9.6	92.8 ± 1.6	90.2 ± 3.3
M262K, A265T, D268Q, H272D, N274E	83.1 ± 5.2	**27.6 ± 1.8**	98.6 ± 3.9
I306T, S316A	**12.1 ± 7.8**	**61.0 ± 1.2**	105.5 ± 3.9

Delineation of the rhodocetin-binding site using mAbs

Previously, a panel of mAbs was raised against the human α2A-domain, and some of their epitopes within the α2A-domain have been mapped [24]. In this study, we also mapped the epitopes of the mAbs JA215, JA218 and JA221, using human–mouse chimaeric α2A-domains. These mAbs recognize the human, but not the murine sequence of the α2A-domain (Table 1). The locations of their epitopes are shown in Figure 5.

By studying the effects of the anti-α2A-domain mAb on $\alpha2\beta1$ integrin binding to immobilized rhodocetin or type I collagen

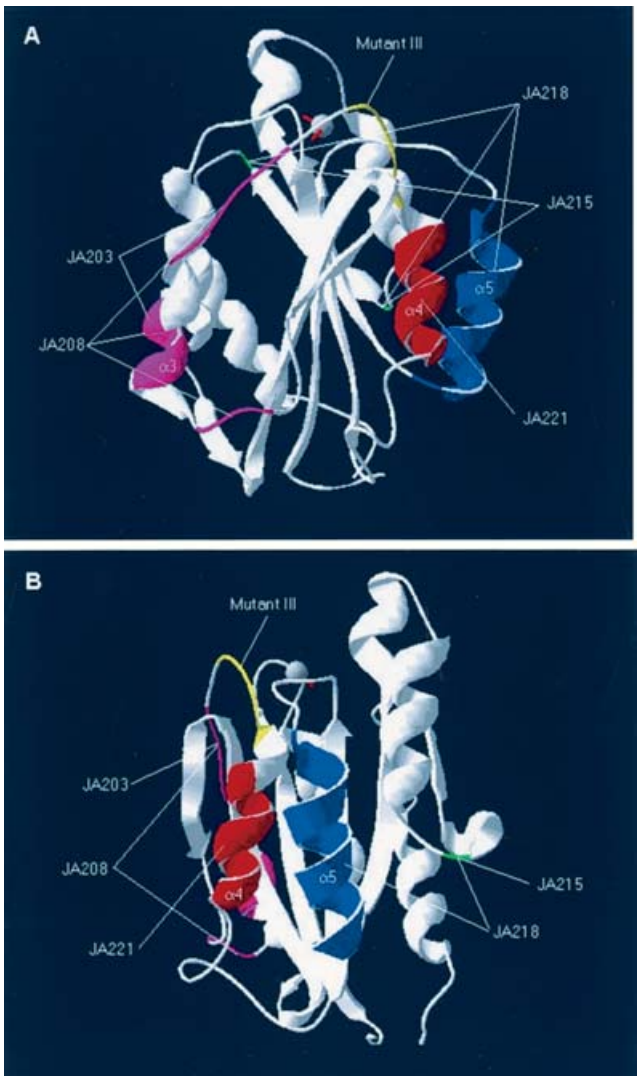

Figure 5 Localization of epitopes of mAbs directed against the α2A-domain and localization of the alanine-substitution mutant III within the α2A-domain

The α2A-domain is viewed from the front **(A)** and from the side after a 90° clockwise rotation around a vertical axis **(B)** with the collagen-binding groove orientated to the top. The helices are labelled. Epitope localization of mAbs JA203, JA208, JA215, JA218 and JA221 within the α2A-domain were mapped as described in the Experimental section. The results are also summarized in Table 1. The location of mutant III within the α2A-domain (mutant III, $Asp^{219} \rightarrow Ala$, $Leu^{220} \rightarrow Ala$, $Asn^{222} \rightarrow Ala$), which affects rhodocetin binding, is marked in yellow.

(Figure 6), we narrowed down the rhodocetin-binding site within the α2A-domain. JA203, which recognizes the C-terminal half of helix α3 and its adjacent C-terminal loop, and JA218, with its non-contiguous epitope on helix α5, and the N- and C-terminal extremities of strand βF (Figure 5), had no effect on $\alpha2\beta1$ integrin binding to either rhodocetin or type I collagen (Figure 6). The antibody JA215 which is directed against the N- and C-terminal extremities of strand βF also did not change rhodocetin binding, but did inhibit type I collagen binding. In contrast, type I collagen binding by soluble $\alpha2\beta1$ integrin was enhanced by the two mAbs JA208 and JA221. JA208 recognizes helix α3 and its adjacent loop regions, and JA221 binds to the C-terminal half of helix α4. Both mAbs increase binding of $\alpha2\beta1$ integrin to collagen. JA208 did not affect rhodocetin binding to the integrin α2A-domain.

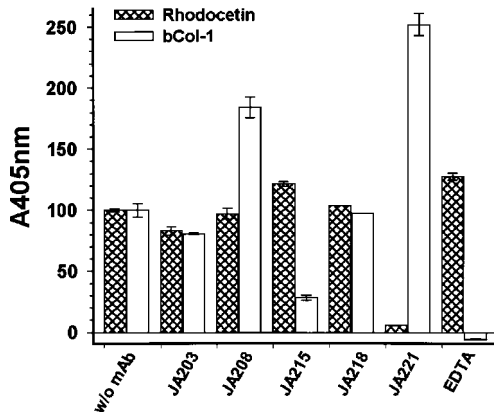

Figure 6 Effect of mAbs directed against the α2A-domain on $\alpha2\beta1$ integrin binding to rhodocetin and type I collagen

Rhodocetin (cross-hatched bars) and bovine type I collagen (open bars) were coated at 20 μg/ml on microtitre plates. Soluble $\alpha2\beta1$ integrin [9 μg/ml in 1 % BSA, TBS (pH 7.4), 2 mM $MgCl_2$ and 1 mM $MnCl_2$] was added either without any antibody (100 % control), or in the presence of a 10-fold molar excess of the indicated mAbs, or in the presence of 10 mM EDTA for 2 h at room temperature. Bound integrin was fixed and quantified by an ELISA, using a rabbit antiserum against the human β1 subunit as primary antibody. Mean values were calculated from duplicate determinations. Values were corrected for non-specific binding signal to BSA-blocked wells and normalized to the mAb-free control.

However, JA221 inhibited the interaction with rhodocetin. This suggests that the JA221 epitope partially or fully overlaps the rhodocetin-binding site of the α2A-domain, which is therefore predicted to be in or proximal to helix α4.

Mapping the rhodocetin-binding site within the α2A-domain by point-mutation analysis

The antibody-inhibition studies were extended by point-mutation analysis of the α2A-domain. Six alanine-substitution mutants were generated in the vicinity of the JA221 epitope, with their location being specified in the Experimental section. Correct folding of the GST-α2A constructs were proven by titration on immobilized mAbs JA218 and JA221, both of which recognize only the native conformation of the α2A-domain (results not shown). All mutants showed binding to mAb JA221, except for mutant IV, which is mutated within the JA221 epitope. All mutants were considered to be correctly folded because all bound to mAb JA218 in a manner comparable with the GST-wild-type α2A, except for mutants II and III, which showed slighly diminshed, yet clear binding signals (results not shown).

GST-α2A was titrated against immobilized rhodocetin (Figure 7A). Mutant III, which corresponds to the α3–α4 loop and the N-terminus of α4 helix (Figure 5), showed dramatically decreased binding to rhodocetin, indicating that this region is part of the rhodocetin-binding site within the α2A-domain. This is consistent with the results obtained above for antibodies. The other alanine mutants could be divided into two groups: the first group comprised mutants II and IV, which showed a titration curve similar to the GST-wild-type α2A construct. Mutants II and IV have alanine substitutions in the βC–α3 loop and the C-terminal part of helix α4, respectively, which are located at the face opposite or distal to the collagen-binding groove of α2A-domain. Significantly, the lack of the effect of mutant IV on rhodocetin binding indicates that the rhodocetin-binding site is proximal to the B-terminal but not to the C-terminal part of the α4-helix region identified as JA221 epitope. The second group of mutants, I, V

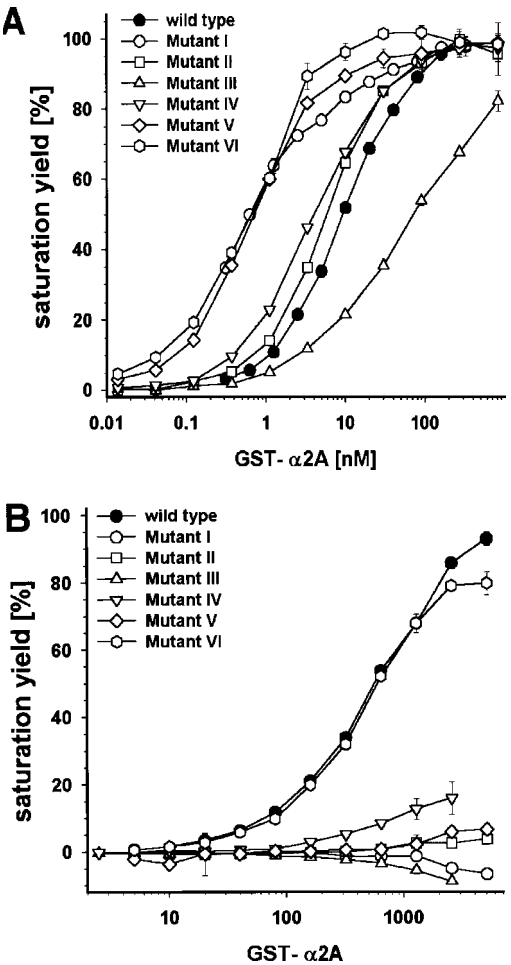

Figure 7 Effect of alanine substitution mutants within the α2A-domain on their binding to rhodocetin and type I collagen

Mutants I–VI were isolated from the bacterial expression system, as detailed in the Experimental section, and tested for the binding capabilities. To this end, rhodocetin (at 20 μg/ml) (**A**) and type I collagen (at 40 μg/ml) (**B**) were immobilized on a microtitre plate at 4 °C, overnight and incubated with the GST-wild-type α2A fusion protein (●) and its mutants I–VI (○, mutant I; □, mutant II; △, mutant III; ▽, mutant IV; ◇, mutant V; ⬡, mutant VI) in 1 % BSA, 50 mM MES/NaOH (pH 6.5), 150 mM NaCl and 2 mM each of $MgCl_2$ and $CaCl_2$ for rhodocetin binding (**A**) or in 1 % BSA, 50 mM Tris/HCl (pH 7.4), 150 mM NaCl and, 2 mM $MgCl_2$ and 1 mM $MnCl_2$ for collagen binding (**B**) for 2 h at room temperature. Bound GST-α2A protein was fixed with a 2.5 % glutaraldehyde solution in 50 mM Hepes/NaOH (pH 7.5), 150 mM NaCl, 2 mM $MgCl_2$ and 1 mM $MnCl_2$ for 10 min and quantified in an ELISA-like procedure, as detailed under the Experimental section. Normalization of the binding signals to the saturation signal of the respective mutant or, in case of non-binding mutants, of the GST-wild-type α2A-fusion protein, yielded the saturation yield. Mean values and standard deviations of duplicate determinations are shown.

and VI, bound with higher affinites to immobilized rhodocetin than the GST-wild-type α2A construct, as their titration curves shifted to lower concentrations of the GST-fusion protein (Figure 7A). Mutant I bears alanine substitutions within the βA–α1 loop, mutant V in the βD–α5 loop and mutant VI in the terminal region of the α5 helix.

Titration of GST-α2A against collagen showed that, despite being correctly folded, all mutants, with the exception of mutant VI, were unable to bind to collagen (Figure 7B). This is consistent with the location of the mutations in I, III and V close to or within the MIDAS. The effects of mutants II and IV on collagen binding may be due to subtle conformational effects on A-domain structure.

Antibody and mutagenesis studies therefore map the rhodocetin-binding site to the α3–α4 loop and the N-terminal part of the α4 helix, a site which overlaps the collagen-binding site as demonstrated both by the absence of collagen binding to mutant III and the fact that the α3–α4 loop residue Thr^{221} belongs to the MIDAS of the α2A-domain. This implies that rhodocetin inhibits collagen binding by steric blocking of the collagen-binding site.

Rhodocetin inhibits collagen binding to $\alpha2\beta1$ integrin in a predominantly competitive manner

An overlap of the rhodocetin- and collagen-binding sites would be expected to result in competitive inhibition. To provide evidence for a competitive inhibition mechanism of rhodocetin, binding curves of $\alpha2\beta1$ integrin to collagen in the presence and absence of rhodocetin were determined. However, fibrillar collagen ligands are rather insoluble and may cause difficulties in binding assays. Therefore, we used the cyanogen bromide-derived fragment CB3 of type IV collagen, which is soluble, yet maintains its essential collagenous triple helix and contains the integrin binding sites for both $\alpha2\beta1$ and $\alpha1\beta1$ integrins [25,26]. Biotinylated, soluble $\alpha2\beta1$ integrin was allowed to bind to CB3 at different concentrations alone or in combination with rhodocetin or in the presence of EDTA. Integrin-bound CB3 was separated from unbound CB3 by pulling it down together with the biotinylated $\alpha2\beta1$ integrin using streptavidin–Sepharose and was eluted with EDTA. The binding curves for the CB3–integrin interaction in the absence of rhodocetin, in the presence of rhodocetin and in the presence of EDTA, are shown in Figure 8(A). After the concentrations of bound CB3 values had been corrected for non-specifically resin-attached CB3, double-reciprocal plots of the specific integrin-bound versus free-CB3 concentrations showed that the curves without and with rhodocetin inhibition converged, indicating a predominantly competitive inhibition by rhodocetin (Figure 8B).

DISCUSSION

Our studies on the mechanism of rhodocetin's activity demonstrated that rhodocetin avidly interacts with the α2A-domain. To our knowledge, rhodocetin is one of the few integrin inhibitors that interacts with an integrin α2 subunit A-domain. Jararhagin from the venom of *Bothrops jararhaga* also binds to $\alpha2\beta1$ integrin and may bind to the α2A-domain [18,19]. Interestingly, a few snake venom toxins have been described which bind to the A1- and A3-domain of the vWF [33], such as botrocetin from *B. jararhaga* [34] and Bitiscetin from *Bitis arietans* [35] respectively. Binding of the toxins induces a conformational change within the vWF A-domain, which eventually enhances the binding of vWF to the receptor GPIb on the platelet surface and results in platelet aggregation. A-domains of integrins and vWF have similar structures and, hence, these snake-venom toxins can be considered as forming a protein family, which not only share sequence similarities but also commonly recognize the A-domain of either vWF or integrin α subunits. Botrocetin and bitiscetin increase the affinity of vWF to the platelet surface resulting in inappropriate blood clotting and thrombus formation, whereas rhodocetin has a converse effect of inhibiting the binding of $\alpha2\beta1$ integrin, the only collagen-binding integrin on the platelet surface. Together with the other collagen-receptor GPVI, $\alpha2\beta1$ integrin plays a key role in collagen-induced platelet aggregation [20]. Therefore, blocking $\alpha2\beta1$ integrin binding to collagen by rhodocetin results in failure of platelet activation [21]. Rhodocetin also acts against $\alpha2\beta1$ integrin on other cell types, affecting other $\alpha2\beta1$ integrin-mediated cellular functions, such as collagen-induced

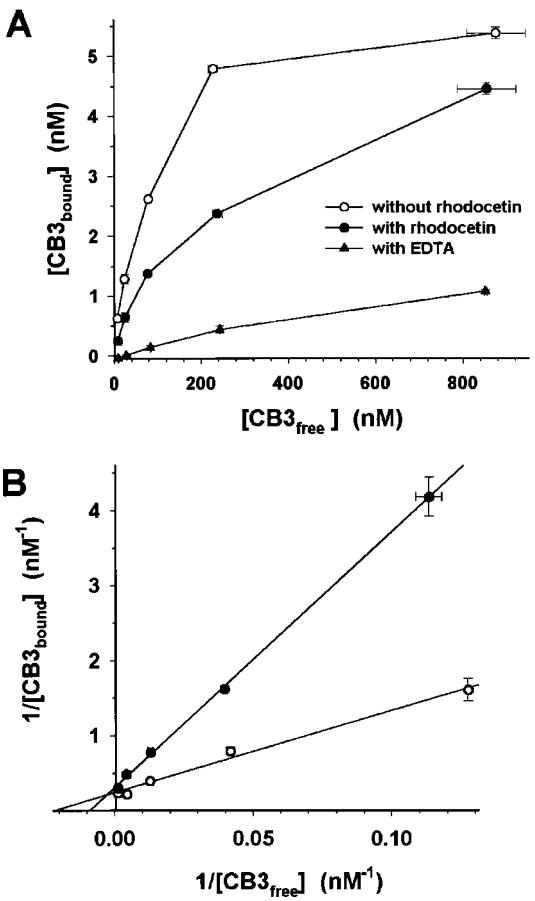

Figure 8 Predominantly competitive manner of rhodocetin inhibition of $\alpha2\beta1$ integrin to type IV collagen fragment CB3

Biotinylated $\alpha2\beta1$ integrin was incubated together with various concentrations of CB3 in both the absence (○) and presence (●) of 32 nM rhodocetin. Integrin-bound CB3 was separated from free CB3 by removing CB3–$\alpha2\beta1$-integrin complexes with streptavidin–agarose. After the loaded resin had been washed four times, integrin-bound CB3 was eluted from the resin with EDTA. To determine non-specific binding of CB3 to the integrin-loaded streptavidin–agarose, the binding assay was also performed in the presence of 10 mM EDTA (▲). Concentrations of free and bound CB3 were quantified using a sandwich ELISA as detailed in the Experimental section. CB3 concentrations were determined in duplicates. Mean values and their standard deviations are shown in the binding curves (**A**). After the binding data had been corrected for non-specific binding, linearization of the binding curves was achieved by double-reciprocal plotting of bound versus free CB3 concentrations (**B**). One out of four independent experiments is shown.

cell attachment and migration, and contraction of collagen gels [23].

The collagen-binding site of $\alpha2\beta1$ integrin has been mapped to the A-domain [7,8], and the interaction of collagen with the $\alpha2$A-domain has been resolved to the molecular level [12,14,15]. The divalent cation, which is required for collagen binding, is complexed on top of the A-domain by residues of three loops, forming the MIDAS: Asp^{140}, Ser^{142} and Ser^{144} in the βA–$\alpha1$ loop, Thr^{209} in the $\alpha3$–$\alpha4$ loop and Asp^{242} in the βD–$\alpha5$ loop. Mutations within these loops abolished collagen binding, as seen here with mutants I, III and V. Further contacts between the collagen main chain and the A-domain involve residues Asn^{154} and Tyr^{157} in the βA–$\alpha1$ loop and His^{258} in the βD–$\alpha5$ loop [12]. Again, mutations of these residues proved detrimental to the capability of $\alpha2$A-domains to bind to collagen, as seen here with mutants I and V. In contrast, a mutation in the central $\alpha5$-helix did not affect collagen binding. By means of these point-mutation analyses and antibody inhibition assays, we mapped the rhodocetin-binding site to the $\alpha3$–$\alpha4$ loop and parts of its adjacent α-helices. This loop contributes to the MIDAS and forms parts of the collagen-binding pocket of the $\alpha2$A-domain. The rhodocetin-binding site therefore overlaps the collagen-binding site, indicating that rhodocetin inhibits by a competitive mechanism. This is consistent with the analysis of binding curves. Interestingly, the $\alpha3$–$\alpha4$ loop is also the interaction site of echovirus 1 [28], but the effect of rhodocetin on echovirus 1 binding has not yet been tested.

An mAb directed against the $\alpha3$–$\alpha4$ loop of the $\alpha1$A-domain has been shown to inhibit collagen binding to $\alpha1\beta1$ integrin, thereby demonstrating that the functional importance of this region is not restricted to the integrin $\alpha2$A-domain. Furthermore, this latter mAb recognizes its epitope in a divalent cation-dependent manner [36]. However, rhodocetin binding to the recombinant $\alpha2$A-domain did not depend on divalent cations, even though the $\alpha3$–$\alpha4$ loop forms a part of MIDAS. Substitution of the integrin-activating Mn^{2+} ions for the Ca^{2+} ions or even their removal by EDTA did not alter the affinity of $\alpha2$A-domain interaction with the integrin inhibitor. This is in contrast with what was seen for the entire $\alpha2\beta1$ integrin ectodomain, the binding of which to rhodocetin was increased by Ca^{2+} ions in a physiological concentration range. Hence, the cation dependence of the A-domain within the entire $\alpha2\beta1$ integrin ectodomain heterodimer must be imposed on it by the rest of the integrin ectodomain. Whether this effect is caused by an alteration of accessibility of $\alpha2$A-domains to rhodocetin or by a conformational change within the $\alpha2$A-domain induced by the rest of the ectodomain, could not entirely be resolved. Significantly, the crystal structure of the integrin $\alpha V\beta3$, which does not have an A-domain, shows a number of Ca^{2+}-binding sites [37]. Homologous sites in the $\alpha2$ and $\beta1$ subunits are, therefore, probable candidates for the sites at which Ca^{2+} regulates rhodocetin and collagen binding.

The $\alpha2$A-domain bound to rhodocetin with an affinity similar to the entire integrin ectodomain heterodimer in the presence of Ca^{2+} ions, suggesting that the isolated $\alpha2$A-domain assumes the less-active conformation. This is supported by the weak binding of the isolated $\alpha2$A-domain to type I collagen in comparison with the $\alpha2\beta1$ ectodomain heterodimer. This suggests that rhodocetin preferentially recognizes the less-active conformation of the $\alpha2$A-domain, and may be a probe which can be used to characterize the conformational state of the $\alpha2$A-domain. Unlike rhodocetin, JA221 recognizes a more active conformation of the A-domain, which is preferentially seen after ligand binding. This antibody is therefore another example of a ligand-induced binding site antibody. Although JA221 and rhodocetin compete sterically in their binding to $\alpha2$A-domain, our results indicate that their overlapping binding sites are likely to undergo a conformational change that affects collagen binding positively and negatively respectively. Independent evidence for this conformational change is seen from comparison of the structures of the liganded and unliganded $\alpha2$A-domain, which shows a displacement of the $\alpha3$–$\alpha4$ loop [12].

Taken together, rhodocetin inhibits collagen-induced, $\alpha2\beta1$ integrin-mediated cell functions on platelets and other cell types, predominantly by competitive inhibition of the collagen-binding site within the $\alpha2\beta1$ integrin. Rhodocetin sterically hinders collagen from entering its binding pocket within the $\alpha2$A-domain by binding to the region of the $\alpha3$–$\alpha4$ loop and the N-terminal part of the $\alpha4$ helix of the $\alpha2$A-domain. Additionally, rhodocetin is likely to induce or maintain the less-active conformation of $\alpha2\beta1$ integrin on the platelet or cell surface. These mechanistic insights into rhodocetin's action explain its antagonistic effects on cells [23], and open new strategies for its use to manipulate collagen-induced cell functions.

We acknowledge the financial support of the Deutsche Forschungsgemeinschaft (grant Eb 177/3-2 to J. A. E.). When this work was carried out, D. T. was supported by a Biotechnology and Biological Sciences Research Council Advanced Research Fellowship (34/AF09035). We thank Alletta Schmidt-Hederich for her excellent technical support. We appreciate the gift of *C. rhodostoma* crude toxin from Dr M. Schwarz (BASF Pharma, Knoll, Ludwigshafen, Germany).

REFERENCES

1 Hynes, R. O. (2002) Integrins: bidirectional, allosteric signaling machines. Cell (Cambridge, Mass.) **110**, 673–687
2 Eble, J. A. (2001) The molecular basis of integrin–extracellular matrix interactions. Osteoarthritis Cartilage **9**, S131–S140
3 Heino, J. (2000) The collagen receptor integrins have distinct ligand recognition and signaling functions. Matrix Biol. **19**, 319–323
4 Eble, J. A. (1997) In Integrin–Ligand Interaction (Eble, J. A. and Kühn, K., eds.), Chapter 1, pp. 1–40, Springer-Verlag, Heidelberg
5 Camper, L., Hellman, U. and Lundgren-Åkerlund, E. (1998) Isolation, cloning, and sequence analysis of the integrin subunit α10, a β1-associated collagen binding integrin expressed on chondrocytes. J. Biol. Chem. **273**, 20383–20389
6 Velling, T., Kusche-Gullberg, M., Sejersen, T. and Gullberg, D. (1999) cDNA cloning and chromosomal localization of human α_{11} integrin, a collagen binding, I domain-containing β_1 associated integrin α-chain present in muscle tissue. J. Biol. Chem. **274**, 25735–25742
7 Tuckwell, D., Calderwood, D. A., Green, L. J. and Humphries, M. J. (1995) Integrin α2 I-domain is a binding site for collagens. J. Cell Sci. **108**, 1629–1637
8 Kamata, T., Puzon, W. and Takada, Y. (1994) Identification of putative ligand binding sites within I domain of integrin $\alpha 2\beta 1$ (VLA-2, CD49b/CD29). J. Biol. Chem. **269**, 9659–9663
9 Eble, J. A., Golbik, R., Mann, K. and Kühn, K. (1993) The $\alpha 1\beta 1$ integrin recognition site of the basement membrane collagen molecule $[\alpha 1(IV)]_2\alpha 2(IV)$. EMBO J. **12**, 4795–4802
10 Knight, C. G., Morton, L. F., Onley, D. J., Peachey, A. R., Messen, A. J., Smethurst, P. A., Tuckwell, D. S., Farndale, R. W. and Barnes, M. J. (1998) Identification in collagen type I of an integrin $\alpha_2\beta_1$-binding site containing an essential GER-sequence. J. Biol. Chem. **273**, 33287–33294
11 Xiong, J.-P., Stehle, T., Zhang, R., Joachimiak, A., Frech, M., Goodman, S. and Arnaout, M. A. (2002) Crystal structure of the extracellular segment of integrin $\alpha V\beta 3$ in complex with Arg-Gly-Asp ligand. Science **296**, 151–155
12 Emsley, J., Knight, C. G., Farndale, R. W., Barnes, M. J. and Liddington, R. C. (2000) Structural basis of collagen recognition by integrin $\alpha 2\beta 1$. Cell (Cambridge, Mass.) **100**, 47–56
13 Arnaout, M. A., Goodman, S. L. and Xiong, J.-P. (2002) Coming to grips with integrin binding to ligands. Curr. Opin. Cell Biol. **14**, 641–651
14 Humphries, M. J. (2002) Insights into integrin–ligand binding and activation from the first crystal structure. Arthr. Res. **4** (Suppl. 3), S69–S78
15 Emsley, J., King, S. L., Bergelson, J. M. and Liddington, R. C. (1997) Crystal structure of the I domain from integrin $\alpha 2\beta 1$. J. Biol. Chem. **272**, 28512–28517
16 White, J. M., Bigler, D., Chem, M., Takahashi, Y. and Wolfsberg, T. G. (2001) In Cell Adhesion, vol. 39 (Beckerle, M. C., ed.), Chapter 6, pp. 189–216, Oxford University Press, Oxford
17 Eble, J. A., Beermann, B., Hinz, H.-J. and Schmidt-Hederich, A. (2001) $\alpha_2\beta_1$ integrin is not recognized by rhodocytin but is the specific high affinity target of rhodocetin, an RGD-independent disintegrin and potent inhibitor of cell adhesion to collagen. J. Biol. Chem. **276**, 12274–12284
18 De Luca, M., Ward, C. M., Ohmori, K., Andrews, R. K. and Berndt, M. C. (1995) Jararhagin and jaracetin: novel snake venom inhibitors of the integrin collagen receptor, $\alpha_2\beta_1$. Biochem. Biophys. Res. Commun. **206**, 570–576
19 Kamiguti, A. S., Hay, C. R. and Zuzel, M. (1996) Inhibition of collagen-induced platelet aggregation as the result of cleavage of $\alpha 2\beta 1$-integrin by the snake venom metalloprotease jararhagin. Biochem. J. **320**, 635–641
20 Moroi, M. and Jung, S. M. (1997) Platelet receptors for collagen. Thromb. Haemostasis **78**, 439–444
21 Wang, R., Kini, R. M. and Chung, M. C. M. (1999) Rhodocetin, a novel platelet aggregation inhibitor from the venom of *Calloselasma rhodostoma* (Malayan pit viper): synergistic and noncovalent interaction between its subunits. Biochemistry **38**, 7584–7593
22 Santoro, S. A. and Zutter, M. M. (1995) The $\alpha_2\beta_1$ integrin: a collagen receptor on platelets and other cells. Thromb. Haemostasis **74**, 813–821
23 Eble, J. A., Niland, S., Dennes, A., Schmidt-Hederich, A., Bruckner, P. and Brunner, G. (2002) Rhodocetin antagonizes stromal tumor invasion *in vitro* and other $\alpha 2\beta 1$ integrin-mediated cell functions. Matrix Biol. **21**, 545–556
24 Tuckwell, D. S., Smith, L., Korda, M., Askari, J. A., Santoso, S., Barnes, M. J., Farndale, R. W. and Humphries, M. J. (2000) Monoclonal antibodies identify residues 199–216 of the integrin α2 vWFA domain as a functionally important region within $\alpha 2\beta 1$. Biochem. J. **350**, 485–493
25 Vandenberg, P., Kern, A., Ries, A., Luckenbill-Edds, L., Mann, K. and Klaus, K. (1991) Characterization of a type IV collagen major cell binding site with affinity to the $\alpha 1\beta 1$ and $\alpha 2\beta 1$ integrin. J. Cell Biol. **113**, 1475–1483
26 Kern, A., Eble, J., Golbik, R. and Kühn, K. (1993) Interaction of type IV collagen with the isolated integrins $\alpha 1\beta 1$ and $\alpha 2\beta 1$. Eur. J. Biochem. **215**, 151–159
27 Heyn, M. P. and Weischet, W. O. (1975) Circular dichroism and fluorescence studies on the binding of ligands to the α subunit of tryphtophan synthase. Biochemistry **14**, 2447–2453
28 King, S. L., Kamat, T., Cunningham, J. A., Emsley, J., Liddington, R. C., Takada, Y. and Bergelson, J. M. (1997) Echovirus 1 interaction with the human very late antigen-2 (integrin $\alpha 2\beta 1$) I domain. J. Biol. Chem. **272**, 28518–28522
29 Brookman, J. L., Stott, A. L., Cheeseman, P. J., Burns, N. R., Adams, S. E., Kingsman, A. J. and Gull, K. (1995) An immunological analysis of the Ty virus-like particle. Virology **207**, 59–67
30 Tuckwell, D. S., Reid, K. B. M., Barnes, M. J. and Humphries, M. J. (1996) Integrin α2 A-domain binds specifically to a range of collagens but is not a general receptor for the collagenous motif. Eur. J. Biochem. **241**, 732–739
31 Lenter, M., Uhlig, H., Hamann, A., Jenö, P., Imhof, B. and Vestweber, D. (1993) A monoclonal antibody against an activation epitope on mouse integrin chain β1 blocks adhesion of lymphocytes to the endothelial integrin $\alpha 6\beta 1$. Proc. Natl. Acad. Sci. U.S.A. **90**, 9051–9055
32 Wilkins, J. A., Li, A., Ni, H., Stupack, D. and Shen, C. (1996) Control of β_1 integrin function, localization of stimulatory epitopes. J. Biol. Chem. **271**, 3046–3051
33 Andrews, R. K. and Berndt, M. C. (2000) Snake venom modulators of platelet adhesion receptors and their ligands. Toxicon **38**, 775–791
34 Sugimoto, M., Mohri, H., McClintock, R. A. and Ruggeri, Z. M. (1991) Identification of discontinuous von Willebrand factor sequences involved in complex formation with botrocetin; a model for the regulation of von Willebrand factor binding to platelet glycoprotein Ib. J. Biol. Chem. **266**, 18172–18178
35 Obert, B., Houllier, A., Meyer, D. and Girma, J.-P. (1999) Conformational changes in the A3 domain of von Willebrand factor modulate the interaction of the A1 domain with platelet gylcoprotein Ib. Blood **93**, 1959–1968
36 Gotwals, P. J., Chi-Rosso, G., Ryan, S. T., Sizing, I., Zafari, M., Benjamin, C., Singh, J., Venyaminov, S. Y., Pepinsky, R. B. and Koteliansky, V. (1999) Divalent cations stabilize the $\alpha 1\beta 1$ integrin I domain. Biochemistry **38**, 8280–8288
37 Xiong, J.-P., Stehle, T., Diefenbach, B., Zhang, R., Dunker, R., Scott, D. L., Joachimiak, A., Goodman, S. L. and Arnaout, M. A. (2001) Crystal structure of the extracellular segment of integrin $\alpha V\beta 3$. Science **294**, 339–345

Received 7 March 2003/25 June 2003; accepted 21 July 2003
Published as BJ Immediate Publication 21 July 2003, DOI 10.1042/ BJ20030373